

# Finite Element Methods for Fractional PDEs in Three Dimensions

Zongze Yang, Yufeng Nie, Zhanbin Yuan, Jungang Wang\*

Department of Applied Mathematics, Northwestern Polytechnical University, Xi'an, Shaanxi 710072, China

---

## Abstract

This paper is a generalization of the previous work (Yang et.al, J. Comput. Phys. 330 (2017), 863–883) to the 3-D irregular convex domains. The analytical calculation formula of fractional derivatives of finite element basis functions are given and a path searching method is developed to find the integration paths corresponding to the Gaussian points. Moreover, a template matrix is introduced to speed up the procedures. Numerical experiments on a steady problem are presented verifying the efficiency of proposed techniques.

*Keywords:* finite element method, fractional derivatives, three dimensions, irregular domains, path searching method,

---

## 1. Introduction

Fractional calculus has been widely used as a modeling tool in numerous fields for diverse applications. However, due to their non-local properties, it is difficult to get closed form or numerical solutions of fractional partial differential equations, especially on the irregular domains in high dimensions. Based on the theoretical and computational framework [3, 4, 8] developed by Ervin and Roop, Zhao et al.[10] developed finite element method for two-dimensional space-fractional advection-dispersion equations. Yang et al.[9] proposed a finite element method(FEM) on unstructured meshes for nonlinear Riesz fractional partial differential equations(FPDEs) in two-dimensional(2-D) domains. Furthermore, Fan et al.[5, 6] solved the time-space fractional wave equation and fractional Schrödinger equation using unstructured meshes. Dehghan and Abbaszadeh [1, 2] studied the finite element solutions for space-multi-time fractional Bloch-Torrey equations and tempered fractional diffusion-wave equations. Though there are so many works on FEM for FPDEs, most of them focus on 1-D or 2-D problems. FPDEs on three-dimensional(3-D) domains are seldom solved by FEM in literature. The main purpose of this work is to extend FEM on unstructured meshes to solve FPDEs on 3-D irregular domains.

Let  $\mathbf{x} = (x_1, \dots, x_n)^T$ ,  $\mathbf{y} = (y_1, \dots, y_n)^T$  be points in  $\mathbb{R}^n$  and  $\mathbf{e}_i (i = 1, 2, \dots, n)$  be the  $i$ -th unit column vector where  $n = 2$  or  $3$ . The boundary of a convex domain  $\Omega$  can be characterized by  $a_i(\mathbf{x})$  and  $b_i(\mathbf{x})$  as below,

$$\begin{aligned} a_i(\mathbf{x}) &:= \inf\{y_i | \mathbf{y} = \mathbf{x} + k\mathbf{e}_i, \mathbf{y} \in \Omega, k \in \mathbb{R}\}, \\ b_i(\mathbf{x}) &:= \sup\{y_i | \mathbf{y} = \mathbf{x} + k\mathbf{e}_i, \mathbf{y} \in \Omega, k \in \mathbb{R}\}. \end{aligned} \quad (1)$$

Here,  $a_i(\mathbf{x})$  and  $b_i(\mathbf{x})$  respectively represent the lower and upper bounds of the line segment parallel to  $\mathbf{e}_i$  through point  $\mathbf{x}$ .

**Definition 1.** Let  $\alpha > 0$ ,  $f(\mathbf{x}) \in L_1(\Omega)$ . Then the left and right Riemann-Liouville fractional integral operators  ${}_{a_i(\mathbf{x})}I_{x_i}^\alpha$  and  ${}_{x_i}I_{b_i(\mathbf{x})}^\alpha$  of order  $\alpha > 0$  with respect to  $x_i$  are defined by

$${}_{a_i(\mathbf{x})}I_{x_i}^\alpha f(\mathbf{x}) := \frac{1}{\Gamma(\alpha)} \int_{a_i(\mathbf{x})}^{x_i} (x_i - y_i)^{\alpha-1} f(\mathbf{x} + (y_i - x_i)\mathbf{e}_i) dy_i, \quad (2)$$

$${}_{x_i}I_{b_i(\mathbf{x})}^\alpha f(\mathbf{x}) := \frac{1}{\Gamma(\alpha)} \int_{x_i}^{b_i(\mathbf{x})} (y_i - x_i)^{\alpha-1} f(\mathbf{x} + (y_i - x_i)\mathbf{e}_i) dy_i. \quad (3)$$

---

\*Corresponding author

Email address: wangjungang@nwpu.edu.cn (Jungang Wang)

**Definition 2.** Let  $m-1 < \alpha < m, m \in \mathbb{N}_+$ . Then the left and right Riemann-Liouville fractional derivatives of  $f(\mathbf{x})$  of order  $\alpha$  with respect to  $x_i$  are defined by

$$\begin{aligned} {}_{a_i(\mathbf{x})}^{\text{RL}}\mathcal{D}_{x_i}^\alpha f(\mathbf{x}) &:= \frac{d^m}{dx_i^m} {}_{a_i(\mathbf{x})}I_{x_i}^{m-\alpha} f(\mathbf{x}), \\ {}_{x_i}^{\text{RL}}\mathcal{D}_{b_i(\mathbf{x})}^\alpha f(\mathbf{x}) &:= (-1)^m \frac{d^m}{dx_i^m} I_{b_i(\mathbf{x})}^{m-\alpha} f(\mathbf{x}). \end{aligned} \quad (4)$$

Fractional differential operators in application mainly contain three forms:  $c(\mathbf{x})\mathcal{D}_i^{2\mu}u(\mathbf{x})$ ,  $\mathcal{D}_i(c(\mathbf{x})\mathcal{D}_i^\nu u(\mathbf{x}))$  or  $\mathcal{D}_i^\nu(c(\mathbf{x})\mathcal{D}_i u(\mathbf{x}))$ , where  $1/2 < \mu < 1, 0 < \nu < 1$ , and  $\mathcal{D}_i^\gamma (\gamma > 0)$  is left or right Riemann-Liouville fractional derivative operator with respect to  $x_i$ , and  $\mathcal{D}_i$  is an abbreviation of classical first order derivative operator  $\frac{\partial}{\partial x_i}$ . When  $u(\mathbf{x})$  is zero on the boundary, the variational forms of those three cases have a uniform form

$$(c(\mathbf{x})\mathcal{D}_i^\alpha u(\mathbf{x}), \hat{\mathcal{D}}_i^\beta v(\mathbf{x})), \quad (5)$$

where  $\alpha, \beta \geq 0, \alpha + \beta = 2\mu$  (or  $\alpha + \beta = 1 + \nu$  for the last two forms), and  $\hat{\mathcal{D}}_i^\beta$  represents the right (left) fractional operator with respect to  $x_i$  if  $\mathcal{D}_i^\alpha$  represents the left (right) fractional operator.

In this paper, we mainly discuss how to assemble stiffness matrix for (5). From (4), we know that the calculation of fractional derivatives of finite element basis functions contain integrals over the lines connecting the Gaussian points to the boundary along the  $i$ -th direction which we call the *integration path* in the following. This is the main challenge in the implementation of FEM for FPDEs and will be discussed in detail in next section. The second section also includes finding the integration paths and some speed-up techniques. In the last section, the proposed methods are applied to solve 3-D steady fractional problems.

## 2. Assembling the fractional stiffness matrix of $(c(\mathbf{x})\mathcal{D}_i^\alpha u(\mathbf{x}), \hat{\mathcal{D}}_i^\beta v(\mathbf{x}))$

Assembling the fractional stiffness matrix is the key point to solve FPDEs using FEM. In this section, we first deduce the analytical calculation formula of fractional derivatives of finite element basis functions. Then, we present the method of finding the integration paths for Gaussian points. Finally, some speed-up techniques are discussed.

### 2.1. Deduction of the analytical formula of fractional derivative of FE basis functions

Assume the domain  $\Omega \in \mathbb{R}^n$  is a polygonal domain which can be partitioned into simplexes in  $\mathbb{R}^n$ . Let  $\{\mathcal{T}_h\}$  be a family of regular partitions of  $\Omega$ , and  $h$  be the maximum diameter of elements in  $\mathcal{T}_h$ . For finite element methods, the idea is to approximate solutions of equations in finite dimensional spaces. So we define the test and trial space  $V_h = \{v_h : v_h \in C(\Omega), v_h \in V, v_h|_E \in P_s(E), \forall E \in \mathcal{T}_h\}$ , where  $P_s(E)$  is the set of polynomials of degree  $\leq s$  in  $E$ . Denote the basis functions of  $V_h$  as  $\psi_l(\mathbf{x}), l = 1, 2, \dots, \mathcal{N}$ . The stiffness matrix can be calculated by adding the element stiffness matrices, i.e.,

$$K = \sum_{E \in \mathcal{T}_h} K_E, \quad (6)$$

where  $K_E$  is element stiffness matrix with  $(K_E)_{kl} = (c(\mathbf{x})\mathcal{D}_i^\alpha \psi_l(\mathbf{x}), \hat{\mathcal{D}}_i^\beta \psi_k(\mathbf{x}))_E$  in which  $(\cdot, \cdot)_E$  represents the  $L^2$  inner product on element  $E$ .

By Gaussian quadrature on  $E$ , we can approximate  $(K_E)_{kl}$  by

$$(K_E)_{kl} = \sum_{j=1}^m w_j c(\mathbf{x}_j) \mathcal{D}_i^\alpha \psi_l(\mathbf{x}_j) \hat{\mathcal{D}}_i^\beta \psi_k(\mathbf{x}_j), \quad (7)$$

where  $\mathbf{x}_j$  and  $w_j$  ( $j = 1, 2, \dots, m$ ) are points and weights of Gaussian quadrature rule on  $E$ .

We take the left Riemann-Liouville fractional operator as an example and suppose we have found the integration path for Gaussian point  $\mathbf{x}$ . Denote  $s_k (k = 1, 2, \dots, p)$  the segments of the integral path, see Fig. 1. And assume  $s_k$  is in element  $E_k$ . Then we have

$$\mathcal{D}_i^\alpha \psi_l(\mathbf{x}) = \frac{1}{\Gamma(1-\alpha)} \frac{d}{dx_i} \int_{a_i(\mathbf{x})}^{x_i} (x_i - y_i)^{-\alpha} \psi_l(\mathbf{y}) dy_i = \sum_{k=1}^p \mathcal{D}_{i,s_k}^\alpha \psi_l(\mathbf{x}), \quad (8)$$

where  $\mathbf{y} = \mathbf{x} + (y_i - x_i)\mathbf{e}_i$  and

$$\mathcal{D}_{i,s_k}^\alpha \psi_l(\mathbf{x}) := \frac{1}{\Gamma(1-\alpha)} \frac{d}{dx_i} \int_{s_k} (x_i - y_i)^{-\alpha} \psi_l(\mathbf{y}) dy_i. \quad (9)$$

From the definition of  $\mathcal{D}_{i,s_k}^\alpha \psi_l(\mathbf{x})$ , we know that if  $\psi_l$  is not a local basis function on  $E_k$ , i.e.  $\psi_l$  is zero on  $s_k$ , we have  $\mathcal{D}_{i,s_k}^\alpha \psi_l(\mathbf{x}) = 0$ . So, we only need to compute  $\mathcal{D}_{i,s_k}^\alpha \psi_l^{(k)}(\mathbf{x})$  where  $\psi_l^{(k)} (l = 1, 2, \dots, n+1)$  are local basis functions on  $E_k$ . In this way, we can calculate the element stiffness matrix locally.

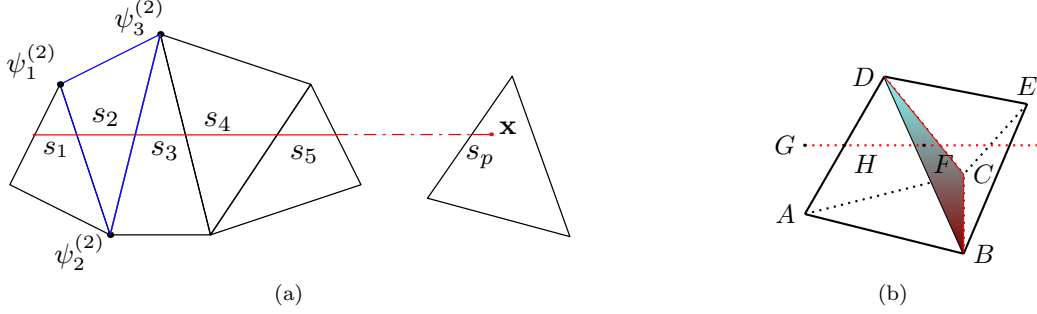


Figure 1: (a). Path of integration for Gaussian point  $\mathbf{x}$  on 2-D domain.  $s_k (k = 1, 2, \dots, p)$  are the segments of the integral path.  $\psi_1^{(2)}, \psi_2^{(2)}, \psi_3^{(2)}$  are local basis functions in  $E_2$ . (b). Path of integration across two elements in 3-D.

## 2.2. Searching the integration paths for Gaussian points

The integration paths consist of intersection segments of elements with the rays starting from Gaussian points along a certain direction. Most existing algorithms for searching the integration paths are exhaustive, i.e. computing the intersection segments of the ray with most of the elements, even every element in the mesh. In [9], we introduced the effect domain to reduce the computation time. Here, we provide another way to accelerate the computation by the ray-simplex intersection algorithm. The key idea of this algorithm is to represent the ray in a new coordinate system related to the simplex [7, Chapter 2].

Denote the ray and the simplex as  $R$  and  $S$ , separately. Assume the vertexes of simplex  $S$  are  $\mathbf{v}_i (i = 0, \dots, n)$  and set  $\tilde{\mathbf{e}}_i = \mathbf{v}_i - \mathbf{v}_0 (i = 1, \dots, n)$ . It is easy to see that  $\{\tilde{\mathbf{e}}_i\}_{i=1}^n$  forms a basis for  $\mathbb{R}^n$ . Hence, every point in simplex  $S$  can be expressed as

$$\mathbf{x} = \mathbf{v}_0 + k_1 \tilde{\mathbf{e}}_1 + k_2 \tilde{\mathbf{e}}_2 + \dots + k_n \tilde{\mathbf{e}}_n, \quad (10)$$

where

$$\begin{cases} k_i \geq 0, \\ k_0 := 1 - \sum_{i=1}^n k_i \geq 0. \end{cases} \quad (11)$$

If we set  $\tilde{\mathbf{k}} = (k_0, k_1, \dots, k_n)^T$ , then  $\tilde{\mathbf{k}}$  is the volume coordinate of  $\mathbf{x}$  in the simplex. Let  $\mathbf{u}_0$  be the start point of  $R$  and  $\mathbf{d} (|\mathbf{d}| = 1)$  be the direction of  $R$ , then every point on ray  $R$  can be written as

$$\mathbf{x} = \mathbf{u}_0 + r\mathbf{d}, \quad r \geq 0. \quad (12)$$

Let  $A = (\tilde{\mathbf{e}}_1, \tilde{\mathbf{e}}_2, \dots, \tilde{\mathbf{e}}_n)$ ,  $\mathbf{k} = (k_1, k_2, \dots, k_n)^T$ ,  $\mathbf{b} = \mathbf{u}_0 - \mathbf{v}_0$ . If  $\mathbf{x}$  is an intersection point of  $S$  and  $R$ , we have

$$\mathbf{A}\mathbf{k} = \mathbf{b} + r\mathbf{d}, \quad r \geq 0, \quad k_i \geq 0 \quad (i = 1, 2, \dots, n),$$

i.e.

$$\mathbf{k} = A^{-1}\mathbf{b} + rA^{-1}\mathbf{d}, \quad r \geq 0, \quad k_i \geq 0 \quad (i = 1, 2, \dots, n). \quad (13)$$

Inserting (13) into (11), we obtain the intersection conditions including only unknown variable  $r$  as below

$$\begin{cases} r \geq 0, \\ \tilde{\mathbf{b}} + r\tilde{\mathbf{d}} \geq \mathbf{0}, \end{cases} \quad (14)$$

where the operator ‘ $\geq$ ’ is element-wise and

$$\tilde{\mathbf{b}} = \begin{pmatrix} A^{-1}\mathbf{b} \\ 1 - \mathbf{e}^T A^{-1}\mathbf{b} \end{pmatrix}, \quad \tilde{\mathbf{d}} = \begin{pmatrix} A^{-1}\mathbf{d} \\ -\mathbf{e}^T A^{-1}\mathbf{d} \end{pmatrix}, \quad (15)$$

where  $\mathbf{e} = (1, 1, \dots, 1)^T$ .

Now, the intersection segment can be derived by solving inequalities (14). Actually, we only need to know the maximum and the minimum  $r$  satisfying (14). Let  $I$  be the set of all  $r$  satisfying (14). If  $I$  is empty or contains only one point,  $I$  has no contribution to the integral. Otherwise,  $I$  is an interval, i.e.  $I = [r_{\min}, r_{\max}]$ ,  $r_{\min} < r_{\max}$ . Therefore, the two end points of the intersection segment are

$$\mathbf{x}_0 = \mathbf{u}_0 + r_{\min}\mathbf{d}, \quad \mathbf{x}_1 = \mathbf{u}_0 + r_{\max}\mathbf{d}, \quad (16)$$

where  $\mathbf{x}_1$  is the go-out point of  $R$  from simplex  $S$ . The volume coordinates of  $\mathbf{x}_0$  and  $\mathbf{x}_1$  can be written as

$$\tilde{\mathbf{k}}_{\min} = \tilde{\mathbf{b}} + r_{\min}\tilde{\mathbf{d}}, \quad \tilde{\mathbf{k}}_{\max} = \tilde{\mathbf{b}} + r_{\max}\tilde{\mathbf{d}}. \quad (17)$$

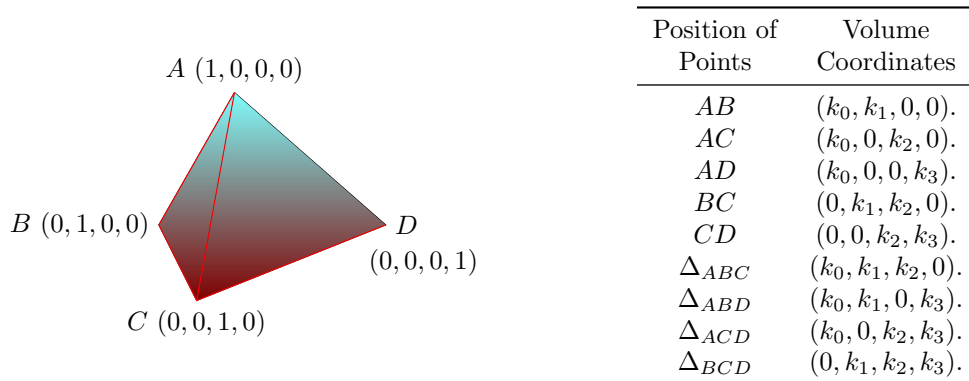


Figure 2: The volume coordinates of nodes and points on edges and faces in tetrahedron.

Assume we have known the adjacent information of the triangulation. If a ray intersects with a simplex  $\Delta$ , then it must go out from some point on some  $m$ -face ( $0 \leq m < n, m \in \mathbb{N}$ ) of the simplex  $\Delta$ , for example, edge(1-face), vertex(0-face) in 2-D case, and face(2-face), edge(1-face), vertex(0-face) in 3-D case. By the volume coordinate of the go-out point, we can get the simplex with which the ray intersect after going out of current simplex. *If the volume coordinate of one point has  $k$  zero components, then the point must be on some  $(n - k)$ -face of the simplex. And the exact face can be determined by the distribution of the zero components of the volume coordinate, see Fig. 2 for 3-D case.* If the go-out point is on an  $m$ -face, we can search all the elements (simplex) which contain the  $m$ -face. Usually, most of the go-out points will locate on  $(n - 1)$ -face of the simplex  $\Delta$ , for example, edges in 2-D and faces in 3-D (See Fig. 1b). And in this situation, there are at most one simplex shared the face with simplex  $\Delta$ . This is why this algorithm is of high-efficiency.

### 2.3. Speedup addition of sparse matrix in MATLAB

When assembling the stiffness matrix we need to add element stiffness matrices together. However, this operation will cost much CPU time because of the sparse matrix storage method in MATLAB. In this subsection, we will exploit the sparsity of the fractional stiffness matrix and further use it to speed up the procedure of assembling fractional stiffness matrix.

Here we take equations with Riesz fractional derivatives as an example. Suppose we have a cubic domain with a uniform grid in  $\mathbb{R}^n$  and assume we have  $N$  grid points on each direction. As presented in Table 1, when  $n = 1$ , the stiffness matrix is full. If  $n > 1$ , the matrix is a sparse matrix and the density of the matrix is proportional to  $1/N^{n-1}$ .

To accelerate the operation, we firstly construct a sparse matrix, called template matrix, of which the structure is 'similar' with the result matrix  $K$ . At the beginning of assembling the fractional stiffness matrix, we set  $K = T$ . And then we just add the element stiffness matrix to  $K$  by a C-routine which will save a

Table 1: Density of the stiffness matrix in different dimensions.

Type	1-D	2-D	3-D
Traditional Equ.	$O(1/N)$	$O(1/N^2)$	$O(1/N^3)$
Fractional Equ.	1	$O(1/N)$	$O(1/N^2)$

lot of time. After we finish the assembling process, we subtract  $T$  from  $K$ . Then we obtain the fractional stiffness matrix that we want. The readers can find the C routine at <https://github.com/lrtfm/addsparse>.

Now we briefly describe the idea of constructing the template matrix  $T$ . Assume  $K_{\mathcal{N} \times \mathcal{N}}$  is a fractional stiffness matrix. Then we define template matrix  $T$  of  $K$  as below

$$T_{jk} = \begin{cases} 0, & \text{if } K_{jk} = 0, \\ 1, & \text{if } K_{jk} \neq 0. \end{cases} \quad (18)$$

So, the process of constructing  $T$  is actually to determine whether  $K_{jk}$  is zero. Here, we take  $(c_i(\mathbf{x})\mathcal{D}_i^\alpha u(\mathbf{x}), \hat{\mathcal{D}}_i^\beta v(\mathbf{x}))$  as an example, i.e.  $K_{jk} = (c_i(\mathbf{x})\mathcal{D}_i^\alpha \phi_k(\mathbf{x}), \hat{\mathcal{D}}_i^\beta \phi_j(\mathbf{x}))$  where  $j, k \in \{1, 2, \dots, \mathcal{N}\}$ . As linear Lagrange element is used, we assume the vertex corresponding to basis function  $\phi_j(\mathbf{x})$  is  $\mathbf{z}_j$  and define  $\omega_j$  as the element patch of  $\mathbf{z}_j$ , i.e.  $\omega_j = \cup_{\mathbf{z}_j \in E} E$ . Define the lower and upper bound of  $\omega_j$  in  $\mathbf{e}_i$  direction as

$$\begin{cases} z_{j,min}^{(i)} = \min\{x_i | \mathbf{x} \in \omega_j\}, \\ z_{j,max}^{(i)} = \max\{x_i | \mathbf{x} \in \omega_j\}. \end{cases} \quad (19)$$

According to the definition of fractional derivatives, if  $[z_{j,min}^{(i)}, z_{j,max}^{(i)}] \cap [z_{k,min}^{(i)}, z_{k,max}^{(i)}] = \emptyset$ , the element  $K_{jk}$  and  $K_{kj}$  must be zeros, i.e.  $T_{jk} = T_{kj} = 0$ . Otherwise,  $K_{jk}$  and  $K_{kj}$  are non-zero, i.e.  $T_{jk} = T_{kj} = 1$ .

The efficiency of this algorithm can be seen from Table 2 which shows the time cost of MATLAB built-in function ‘plus’ and C routine ‘addsparse’ in assembling the stiffness matrix of Riesz fractional derivatives. For fractional stiffness matrix, the acceleration effect of ‘addsparse’ is remarkable.

Table 2: Comparison of times cost by MATLAB built-in function ‘plus’ and our C routine ‘addsparse’.

Number of elements	$\alpha = 1$		$\alpha = 0.8$	
	‘addsparse’	‘plus’	‘addsparse’	‘plus’
940	0.06s	0.03s	0.07s	0.07s
2583	0.18s	0.13s	0.29s	0.62s
10746	1.05s	1.52s	1.73s	50.40s
38139	7.52s	20.09s	11.62s	945.53s

### 3. Application

In this section, we will use the methods proposed in previous section to solve the steady fractional diffusion equation with linear finite elements.

Let us consider FPDEs with variable coefficients in divergence form

$$\begin{cases} \sum_{i=1}^3 \mathcal{D}_i \left( p_i(\mathbf{x}) {}_{a_i(\mathbf{x})}^{\text{RL}} \mathcal{D}_{x_i}^{\beta_i} u(\mathbf{x}) - q_i(\mathbf{x}) {}_{x_i}^{\text{RL}} \mathcal{D}_{b_i(\mathbf{x})}^{\beta_i} u(\mathbf{x}) \right) = f(\mathbf{x}), & \mathbf{x} \in \Omega, \\ u(\mathbf{x}) = 0, & \mathbf{x} \in \mathbb{R}^3 \setminus \Omega, \end{cases} \quad (20)$$

where  $p_i(x) > 0, q_i(x) > 0, \Omega = \{\mathbf{x} | |\mathbf{x}| < r\}$  and  $r = 0.5$ . The variational form of this equation is  $a(u, v) = (f, v)$ , where

$$a(u, v) = - \sum_{i=1}^3 \left( (p_i(\mathbf{x}) {}_{a_i(\mathbf{x})}^{\text{RL}} \mathcal{D}_{x_i}^{\beta_i} u, \mathcal{D}_i v) - (q_i(\mathbf{x}) {}_{x_i}^{\text{RL}} \mathcal{D}_{b_i(\mathbf{x})}^{\beta_i} u, \mathcal{D}_i v) \right). \quad (21)$$

Denote  $\beta = (\beta_1, \beta_2, \beta_3)$  and set  $(p_1, p_2, p_3) = (\cos(x_1), \cos(x_2), \cos(x_3))$ ,  $(q_1, q_2, q_3) = (1 - \cos(x_1), 1 - \cos(x_2), 1 - \cos(x_3))$ . Let the exact solution be

$$u(\mathbf{x}) = (x_1^2 + x_2^2 + x_3^2 - r^2)^2, \quad (22)$$

and  $f(\mathbf{x})$  be the corresponding inhomogeneous term obtained by inserting  $u(\mathbf{x})$  into the original equation.

The exact solution and the numerical result with  $h \approx 0.0894166$  are presented in Fig. 3. The errors and convergence orders are shown in Table 3 with  $\beta = (0.8, 0.8, 0.8)$  and  $\beta = (0.6, 0.7, 0.8)$ , separately. According to [3, Theorem 7.3], the theoretical convergence order should be 2 which is consistent with our numerical results.

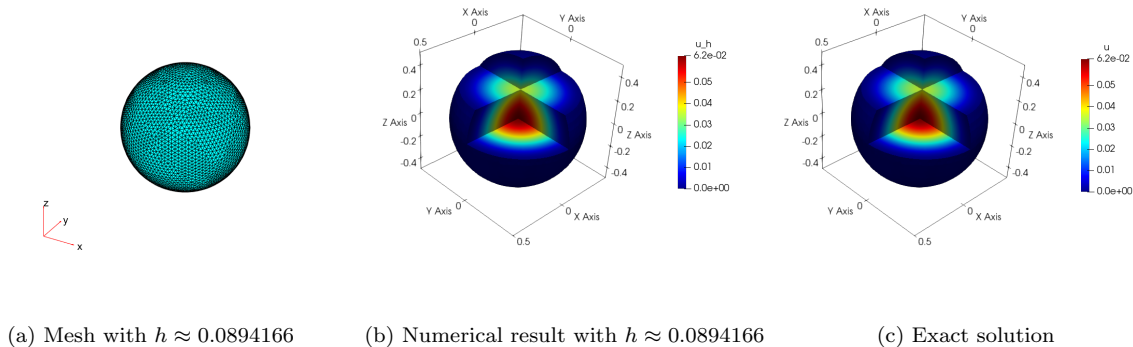


Figure 3: Numerical result and exact solution for (20).

Table 3:  $L^2$  and  $L^\infty$  errors and convergence orders for (20).

Errors $h$	$\beta$ (0.8, 0.8, 0.8)				(0.6, 0.7, 0.8)			
	$\ u - u_h\ _{L^2}$	order	$\ u - u_h\ _{L^\infty}$	order	$\ u - u_h\ _{L^2}$	order	$\ u - u_h\ _{L^\infty}$	order
0.270055	7.79e-04		2.24e-03		7.87e-04		2.30e-03	
0.139416	2.64e-04	1.64	7.53e-04	1.65	2.74e-04	1.60	7.99e-04	1.60
0.0757345	8.05e-05	1.95	2.34e-04	1.91	8.68e-05	1.88	2.85e-04	1.69

## 4. Conclusion

In this paper, we search the integration paths by a ray-simplex algorithm which can speed-up the procedures of assembling fractional stiffness matrices. The algorithm is easy to implement and can be used in any  $n$ -dimensional space. Furthermore, we apply the method to solved 3-D steady fractional problem.

As shown in Table 4, although we propose a valid method on searching integral path and some techniques to speed up the addition of sparse matrix, the assembly of the fractional stiffness matrix is still much slower than that of the integer order stiffness matrix. It is still needed to conduct in-depth research on fast algorithms of assembling fractional stiffness matrix on irregular domains.

## Acknowledgements

This research was supported by the National Natural Science Foundation of China (Grant No.11601432 and No.11971386) and the Fundamental Research Funds for the Central Universities (Grant No.310201911cx025).

The authors would like to thank Professor Fawang Liu of Queensland University of Technology for his helpful comments on an earlier version of this manuscript. The authors would like to thank the anonymous reviewers for their useful comments, which have led to an improvement of the presentation.

Table 4: Comparison of time used in solving fractional and integer elliptic equations

Number of elements	Fractional elliptic equation		Elliptic equation	
	Assemble matrix	Solve linear equations	Assemble matrix	Solve linear equations
4061	35.61s	0.02s	0.92s	0.03s
64740	11m 34.60s	0.52s	8.96s	0.09s
268418	1h 36m 38.75s	8.62s	33.18s	0.73s

## References

- [1] Mehdi Dehghan and Mostafa Abbaszadeh. An efficient technique based on finite difference/finite element method for solution of two-dimensional space/multi-time fractional Bloch–Torrey equations. *Applied Numerical Mathematics*, 131:190–206, 2018.
- [2] Mehdi Dehghan and Mostafa Abbaszadeh. A finite difference/finite element technique with error estimate for space fractional tempered diffusion-wave equation. *Computers & Mathematics with Applications*, 75(8):2903–2914, 2018.
- [3] Vincent J Ervin and John Paul Roop. Variational solution of fractional advection dispersion equations on bounded domains in  $R^d$ . *Numerical Methods for Partial Differential Equations*, 23(2):256, 2007.
- [4] V.J. Ervin and J.P. Roop. Variational formulation for the stationary fractional advection dispersion equation. *Numerical Methods for Partial Differential Equations*, 22(3):558–576, 2006.
- [5] Wenping Fan, Fawang Liu, Xiaoyun Jiang, and Ian Turner. A novel unstructured mesh finite element method for solving the time-space fractional wave equation on a two-dimensional irregular convex domain. *Fractional Calculus and Applied Analysis*, 20(2), 2017.
- [6] Wenping Fan and Haitao Qi. An efficient finite element method for the two-dimensional nonlinear time-space fractional Schrödinger equation on an irregular convex domain. *Applied Mathematics Letters*, 86:103–110, 2018.
- [7] Andrew S Glassner. *An Introduction to Ray Tracing*. Elsevier, 1989.
- [8] John Paul Roop. Computational aspects of FEM approximation of fractional advection dispersion equations on bounded domains in  $R^2$ . *Journal of Computational and Applied Mathematics*, 193(1):243–268, 2006.
- [9] Z. Yang, Z. Yuan, Y. Nie, J. Wang, X. Zhu, and F. Liu. Finite element method for nonlinear Riesz space fractional diffusion equations on irregular domains. *Journal of Computational Physics*, 330:863–883, 2017.
- [10] Yanmin Zhao, Weiping Bu, Jianfei Huang, Da-Yan Liu, Yifa Tang. Finite element method for two-dimensional space-fractional advection-dispersion equations. *Applied Mathematics and Computation*, 257:553–565, 2015.